A Close Examination of Multiple Model Adaptive Estimation Vs Extended Kalman Filter for Precision Attitude Determination

Quang M. Lam[1]
LexerdTek Corporation
Clifton, VA 20214

John L. Crassidis[2]
University at Buffalo, State University of New York
Amherst, NY 14260-4400

To be submitted to the AIAA Space 2013, September 2013. San Diego, CA

Abstract

With today's advanced nonlinear filtering (e.g., Multiple Model Adaptive Estimator, MMAE, or Particle Filter, PF) and noise identification for filter update at the roll-off level (via the Q matrix) and noise cancellation at the measurement level approach a reasonable technology maturation level, it is strongly believed that an extremely high precision attitude determination can be practically achieved using commercial low cost low grade MEMS inertial sensors (i.e., MEMS gyros and accelerometers and/or MEMS IMU). This paper revisits the MMAE design developed in [2] & [7] with a close examination of its performance using high fidelity models of the gyros and star tracker to determine its viability for a possible design and implementation of a new attitude determination system using low cost low grade MEMS gyros (i.e., > 0.035 deg/hr^0.5 and 3deg/hr bias) and CMOS Star Trackers (i.e., >70 arcseconds). The proposed MMAE design with gyros noise identification (i.e., Angular Random Walk (ARW) and Rate Random Walk (RRW) are primary elements to be estimated in real time for update and cancellation) is evaluated against the single EKF based design for a performance measure of how well the proposed MMAE and Noise Identification scheme improves over the baseline design. The design is evaluated using the Matlab based environment.

I. Introduction

[1] Lam.Quang@Lexerdtek.com, Ph.D., CTO
[2] johnc@buffalo.edu, Ph.D., Professor, Department of Mechanical & Aerospace Engineering. Associate Fellow AIAA.

1.1 Understanding MEMS IRU High Noise Nature.

The measured (noisy) angular rate vector, $\tilde{\omega}$, of a Rate Integrating Gyro (RIG) is described by the following equations:

$$\begin{aligned}
\tilde{\boldsymbol{\omega}} &= \left(I_{3\times 3} + S\right)\boldsymbol{\omega} + \mathbf{b} + \boldsymbol{\eta}_v \\
\dot{\mathbf{b}} &= \boldsymbol{\eta}_u \\
\dot{\mathbf{s}} &= \boldsymbol{\eta}_s \\
\dot{\mathbf{k}}_U &= \boldsymbol{\eta}_U \\
\dot{\mathbf{k}}_L &= \boldsymbol{\eta}_L \\
S &\equiv \begin{bmatrix} s_1 & k_{U1} & k_{U2} \\ k_{L1} & s_2 & k_{U3} \\ k_{L2} & k_{L3} & s_3 \end{bmatrix}
\end{aligned} \tag{1.1}$$

where **b** is the bias driven by the RRW, η_u; η_v is the ARW (i.e., the white noise at the rate level and becomes RW at the angle output). The *S* matrix in Eq. (1.1) contains two major error sources, scale factor error s_i and misalignment errors K_{Ui} and K_{Li} where

s_i, i=1,2,3 is the gyro scale factor errors driven by the white noise η_s
K_{Ui} is the upper misalignment errors driven by the white noise η_U
K_{Li} is the lower misalignment errors driven by the white noise η_L

At normal rate operating conditions for space missions (<2 deg/sec slew), the *S* term in equation (2) can be ignored; however, for high rate operating conditions, the *S* term needs to be estimated online in order to cancel out their contributed errors as the product of *S* and **ω**. The larger the rate magnitude is, the larger the scale factor errors and misalignment errors will be. At the current state of practice, only bias errors, $b_{x,y,z}$, are being accounted for at the filtering level as part of the well-known 6 state EKF [1] (i.e., $X_{EKF} = [\theta_x \ \theta_y \ \theta_z \ b_x \ b_y \ b_z]^T$ where $[[\theta_x \ \theta_y \ \theta_z \ ]$ are three Euler angles).

The scale factor errors and misalignment errors are negligible for high quality gyros but for MEMS sensors, they become a dominant noise source "contaminating" the truth rate, thus affecting vehicles' rate loop closure stability for either spacecraft or missile applications. Figure 1 illustrates the effect of the *S* matrix on the EKF estimation accuracy under a high slew rate condition of MEMS gyros.

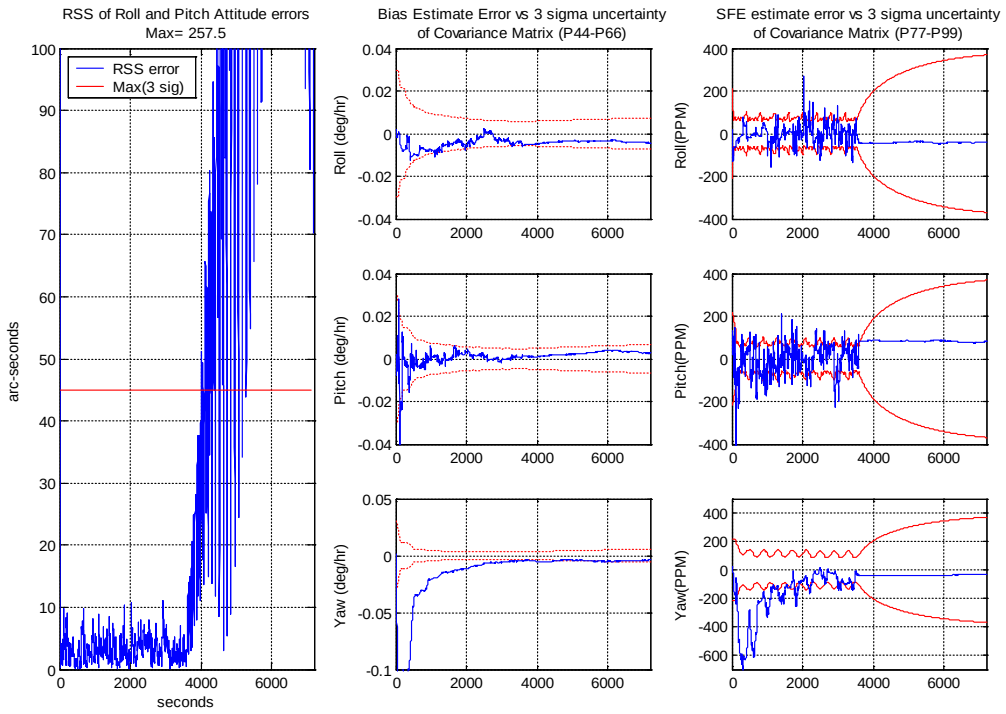

Figure 1: The effect of the *S* matrix under the high rate slew condition and not properly tuned Q matrix. The attitude error (shown on the left) and the bias estimate errors in the yaw axis are not accurately estimated.

Therefore, the ability to accurately predict or estimate S matrix (which is a combination of scale factor errors and misalignment errors) as part of the real time filter's actions is the key to the success of transforming the MEMS inertial sensors into high grade inertial sensors. This implies that the EKF needs to have a 9 state (adding three scale factor errors to the basic 6 state EKF described earlier) or 15 state (adding 6 more misalignment errors to the 9 state) vectors. That has been the design direction to address high rate slew missions [3-4]. However, those directions are still mainly dictated by the fundamental drawbacks of the EKF based design techniques, which are summarized as follows,

- EKF is based on the first-order linearization of the true nonlinear dynamics and measurement equations. Thus, the estimation accuracy and stability will deteriorate under high nonlinearity and large uncertainties.
- The heavy reliance on the prior knowledge of the EKF's state noise covariance matrix (Q) and the measurement noise covariance matrix (R) (see Figure 2), which, in reality, are usually difficult to obtain after deploying them in orbit, makes the EKF vulnerable. All gyro noise parameters are varying on orbit and getting worse after certain duration, thus affecting the value of the Q matrix. Likewise, star tracker as external aiding source to the EKF has its R matrix varied as well.
- If the pair [Q, R] matrices are not properly tuned per operating regime or flight condition, the EKF performance will drastically suffer, thus not being able to provide a navigation solution accurate enough to support the guidance and control loop closures for coordinated commands and actions generation.

- Likewise, the measurement covariance matrix R needs to be tuned not only for the sensor characteristics but also for its bandwidth operating conditions. An adaptive R matrix for EKF has been searched during the past decades; however, none has been seen in the state of practice.
- The fundamental and inherent inappropriate assumption that the pair [Q, R] matrices are uncorrelated and white.

Our proposed concept, leveraging the adaptive filtering design scheme called the Multiple Model Adaptive Estimation (MMAE) coupled with the gyros noise estimation for update and cancellation, is offering a performance characteristic that at this point, via simulation, significantly outperforms the EKF and other modern nonlinear filtering schemes like Unscented Kalman filter (UKF).

1.2 Why Noise Cancellation Will Work

If we examine the gyro output equation (eq. (1)), the key step is to estimate the ARW term for the process noise Q matrix update to reflect its in-orbit operation status and factor them into the filter via the roll-off process since the bias and *S* term can be done via the estimation process (proven steps, see [1-4]). Therefore, the main challenge is the ARW estimation and cancellation. This concept has been identified by several researchers during the past decade (e.g., [3] [5]). We propose a different technique instead of using heuristic approach proposed by [5]. Our concept is illustrated in Figures 3 and 4 below. How the ARW can be estimated and identified in real time is presented in Figure 4. The ARW noise estimation concept has been studied in [5] & [6] and now can be matured and implemented in a practical implementation.

Gyros Noise Isolation and Identification Concept

It is worth pointing out that the gyro's individual noise source isolation and identification proposed is done in a real-time fashion. The characterization of the scale factor (SF) error stability and bias error stability is the key factor to the success of this technique. As depicted in Figures 3 and 4, the characterization of these two noise sources is accomplished by the calibration filter to provide the error correction. Two innovative features that make the overall concept viable are emphasized as follows:

- **Real-Time Statistical Identification of gyros noise sources such as ARW and AWN:** The real-time 1-sigma value identification capability of these white noise sources is critical to the performance maintenance of the calibration filter since the values of these noise sources may be significantly different from the IRU vendor's specification after being deployed on orbit. With the correct statistical knowledge of these white noise sources identifiable in real-time, the calibration filter process noise can be updated in real-time to provide accurate calibration.
- **Real-Time Characterization of Scale Factor Error and Bias Error Stability Variation:** To fully capture the stability variation of the SF error and bias error, either as a random walk or correlated noise process both for symmetric and asymmetric elements, the white noise characteristics that drive the SF error stability or the bias stability need to be constantly monitored and identified in real-time. These values are normally not available from vendor's specification. However, they are important for the filter to achieve acceptable performance for calibration, thereby allowing MEMS IRU utilization

with a more accurate solution.

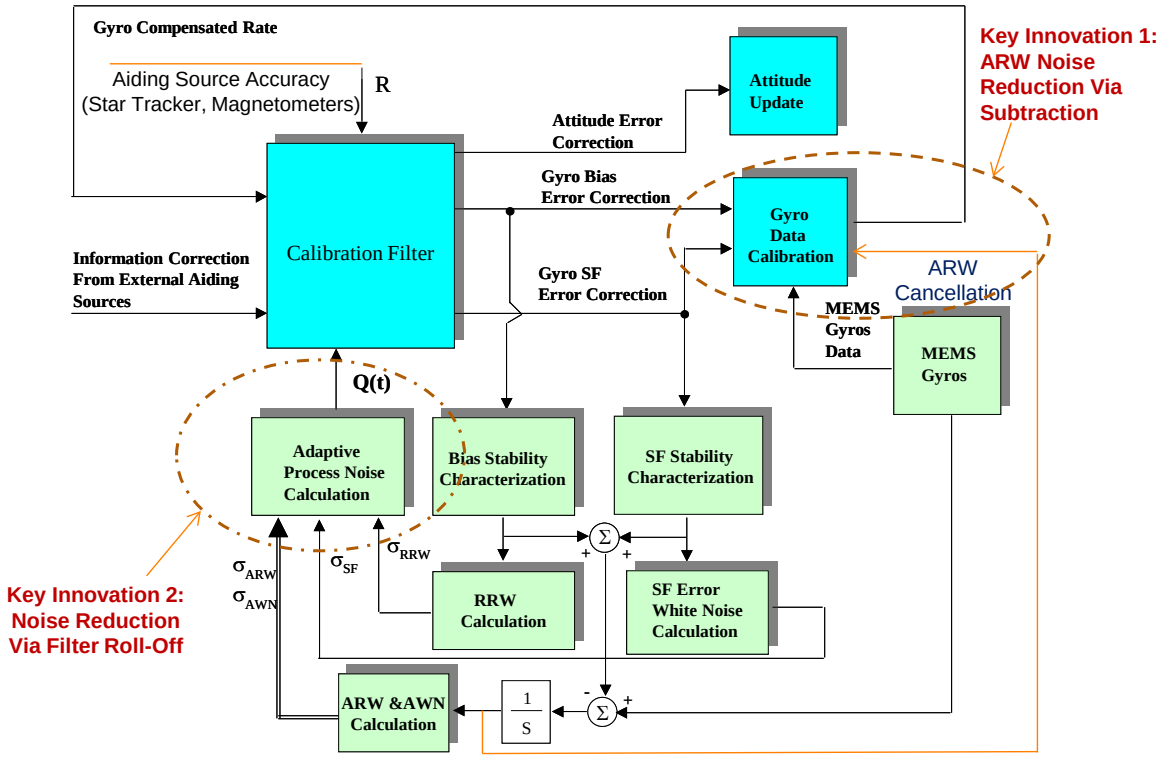

Figure 3: Innovative Calibration and Filtering Architecture Allowing MEMS Inertial Sensors Reaching Navigation Grade

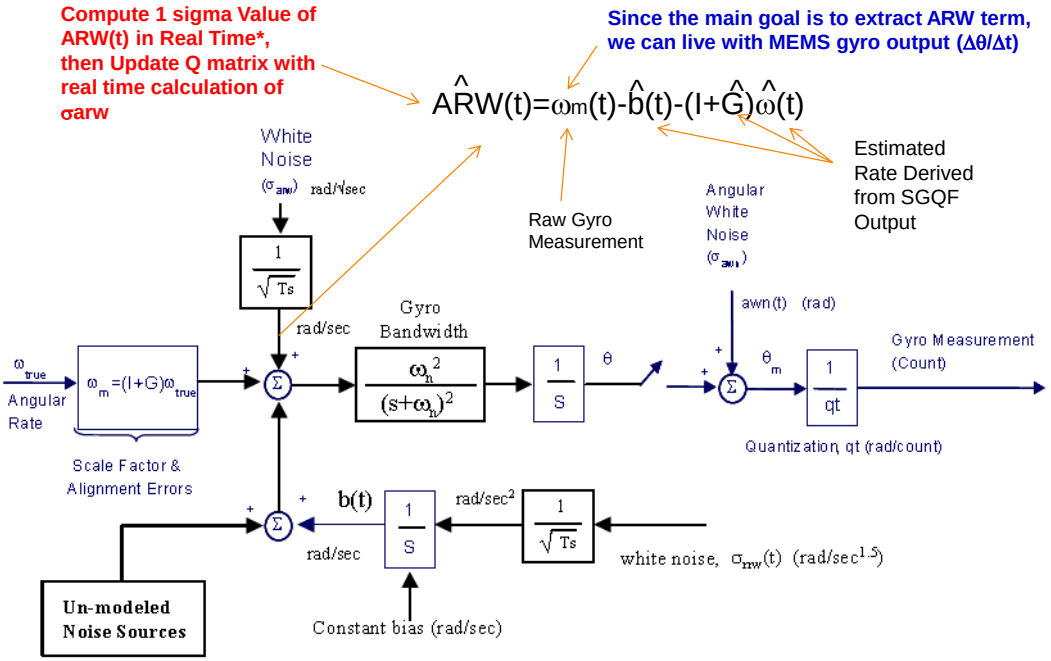

The noise estimation for filter update and cancellation at measurement as simultaneous action concept has been viewed as a popular design trend since 2003; however, the current real time isolation approach presented herein is the most practical and implementable one (over the Allan Variance Analysis which is only good for offline)

Figure 4: Real Time ARW Noise Estimation for Update and Cancellation

These two features will allow the compensation of MEMS IRU in a very unique way as compared to the traditional attitude estimation solution. We employ the correlated noise model (i.e., first order Markov model) described in [5] to capture the bias error and SF error of the gyros for this study.

2.0 Development of a 15 State Extended Kalman Filter

2.1 Quaternion Parameterization and Gyro Model

For spacecraft attitude estimation, the quaternion has been the most widely used attitude parameterization [1]. The quaternion is given by a four-dimensional vector, defined as

$$\mathbf{q} = \begin{bmatrix} \mathbf{q}_{13} \\ q_4 \end{bmatrix} \tag{1}$$

with $\mathbf{q}_{13} \equiv \begin{bmatrix} q_1 & q_2 & q_3 \end{bmatrix}^T = \mathbf{d}\sin(\vartheta/2)$ and $q_4 = \cos(\vartheta/2)$, where $\mathbf{d}$ is the unit Euler axis and ϑ is the rotation angle. Because a four-dimensional vector is used to describe three dimensions, the quaternion components cannot be independent of each other. The quaternion satisfies a single constraint given by $\mathbf{q}^T\mathbf{q} = 1$. The attitude matrix is related to the quaternion by

$$A(\mathbf{q}) = \Xi^T(\mathbf{q})\Psi(\mathbf{q}) \tag{2}$$

with

$$\Xi(\mathbf{q}) \equiv \begin{bmatrix} q_4 I_{3\times 3} + [\mathbf{q}_{13}\times] \\ -\mathbf{q}_{13}^T \end{bmatrix} \tag{3a}$$

$$\Psi(\mathbf{q}) \equiv \begin{bmatrix} q_4 I_{3\times 3} - [\mathbf{q}_{13}\times] \\ -\mathbf{q}_{13}^T \end{bmatrix} \tag{3b}$$

where $I_{3\times 3}$ is a 3×3 identity matrix and $[\mathbf{q}_{13}\times]$ is the cross product matrix, defined by

$$\left[\mathbf{q}_{13}\times\right]\equiv\begin{bmatrix}0 & -q_3 & q_2\\ q_3 & 0 & -q_1\\ -q_2 & q_1 & 0\end{bmatrix} \tag{4}$$

For small angles the vector part of the quaternion is approximately equal to half angles [6].

The quaternion kinematics equation is given by

$$\dot{\mathbf{q}}=\frac{1}{2}\Xi(\mathbf{q})\boldsymbol{\omega} \tag{5}$$

where $\boldsymbol{\omega}$ is the three-component angular rate vector. A major advantage of using the quaternion is that the kinematics equation is linear in the quaternion and is also free of singularities. Another advantage of the quaternion is that successive rotations can be accomplished using quaternion multiplication. Here the convention of [6] is adopted, where the quaternions are multiplied in the same order as the attitude matrix multiplication, in contrast to the usual convention established by Hamilton. A successive rotation is written using $A(\mathbf{q}')A(\mathbf{q})=A(\mathbf{q}'\otimes\mathbf{q})$. The composition of the quaternions is bilinear, with

$$\mathbf{q}'\otimes\mathbf{q}=\left[\Psi(\mathbf{q}') \quad \mathbf{q}'\right]\mathbf{q}=\left[\Xi(\mathbf{q}) \quad \mathbf{q}\right]\mathbf{q}' \tag{6}$$

Also, the inverse quaternion is given by $\mathbf{q}^{-1}\equiv\left[-\mathbf{q}_{13}^T \quad q_4\right]^T$, with $A\left(\mathbf{q}^{-1}\right)=A^T(\mathbf{q})$. Note that $\mathbf{q}\otimes\mathbf{q}^{-1}=\begin{bmatrix}0 & 0 & 0 & 1\end{bmatrix}^T$, which is the identity quaternion.

A common sensor that measures the angular rate is a rate integrating gyro. For this sensor, a widely used three-axis continuous-time model is given by

$$
\begin{aligned}
\tilde{\boldsymbol{\omega}} &= \left(I_{3\times 3} + S\right)\boldsymbol{\omega} + \mathbf{b} + \boldsymbol{\eta}_v \\
\dot{\mathbf{b}} &= \boldsymbol{\eta}_u \\
\dot{\mathbf{s}} &= \boldsymbol{\eta}_s \\
\dot{\mathbf{k}}_U &= \boldsymbol{\eta}_U \\
\dot{\mathbf{k}}_L &= \boldsymbol{\eta}_L \\
S &\equiv \begin{bmatrix} s_1 & k_{U1} & k_{U2} \\ k_{L1} & s_2 & k_{U3} \\ k_{L2} & k_{L3} & s_3 \end{bmatrix}
\end{aligned}
\tag{7}
$$

where $\tilde{\boldsymbol{\omega}}$ is the measured rate, $\mathbf{b}$ is the drift, S is a matrix of scale factors $\mathbf{s}$ and misalignments $\mathbf{k}_U$ and $\mathbf{k}_L$, and $\boldsymbol{\eta}_v$ (i.e., angular random walk, ARW), $\boldsymbol{\eta}_u$ (i.e., rate random walk, RRW) and $\boldsymbol{\eta}_s$, $\boldsymbol{\eta}_U$ and $\boldsymbol{\eta}_L$ are independent zero-mean Gaussian white-noise processes with

$$
\begin{aligned}
E\left\{\boldsymbol{\eta}_v(t)\boldsymbol{\eta}_v^T(\tau)\right\} &= \sigma_v^2\delta(t-\tau)I_{3\times 3} \\
E\left\{\boldsymbol{\eta}_u(t)\boldsymbol{\eta}_u^T(\tau)\right\} &= \sigma_u^2\delta(t-\tau)I_{3\times 3} \\
E\left\{\boldsymbol{\eta}_s(t)\boldsymbol{\eta}_s^T(\tau)\right\} &= \sigma_s^2\delta(t-\tau)I_{3\times 3} \\
E\left\{\boldsymbol{\eta}_U(t)\boldsymbol{\eta}_U^T(\tau)\right\} &= \sigma_U^2\delta(t-\tau)I_{3\times 3} \\
E\left\{\boldsymbol{\eta}_L(t)\boldsymbol{\eta}_L^T(\tau)\right\} &= \sigma_L^2\delta(t-\tau)I_{3\times 3}
\end{aligned}
\tag{8}
$$

where E{ } denotes expectation and $\delta(t-\tau)$ is the Dirac-delta function.

2.2 Kalman Filtering for Attitude Estimation

This section provides a review of the equations involved for spacecraft attitude estimation using the Kalman filter. The measurements are assumed to be given for a star tracker determined Kalman filter. To within first-order the quaternion measurements can be modeled by

$$
\tilde{\mathbf{q}} = \mathbf{q} + \frac{1}{2}\Xi(\mathbf{q})\mathbf{v} \tag{9}
$$

where $\tilde{\mathbf{q}}$ is the measurement quaternion and $\mathbf{v}$ is a zero-mean Gaussian process with covariance R. Note that $\mathbf{v}$ is not a stationary process and R is determined from the attitude error-covariance of the attitude determination process [4]. Also, to within first-order the quaternion normalization constraint is maintained with this measurement model. A summary of the extended Kalman filter (EKF) for attitude estimation, including gyro drifts and scale factors, is shown in Table 1. All symbols and characters with a hat over them signify estimates. The

variables P_k^+ and P_k^- denote the updated and propagated error-covariance at time t_k, respectively; K_k is the Kalman gain; the first three components of $\Delta\hat{\mathbf{x}}$, denoted by $\boldsymbol{\delta}\hat{\boldsymbol{\alpha}}$, are the small-attitude error estimates, and the vector $\hat{\mathbf{s}}$ denotes the diagonal elements of the estimate scale factor matrix, $\hat{S}$. Note that the propagated values for the gyro drift and scale factors are given by their previous time values.

We now derive the $F(t)$ and $G(t)$ matrices. Here it is assumed that $(I_{3\times3}+S)^{-1} \approx (I_{3\times3}-S)$, which is valid for small S. A multiplicative error quaternion is used to derive the attitude errors:

$$\boldsymbol{\delta}\mathbf{q} = \mathbf{q} \otimes \hat{\mathbf{q}}^{-1} \approx \begin{bmatrix} 0.5\boldsymbol{\delta}\boldsymbol{\alpha} \\ 1 \end{bmatrix} \tag{10}$$

where $\boldsymbol{\delta}\boldsymbol{\alpha}$ is the vector of small attitude (roll, pitch and yaw) attitude errors. The error-kinematics follow [1]

$$\dot{\boldsymbol{\delta}}\boldsymbol{\alpha} = -\left[\hat{\boldsymbol{\omega}}\times\right]\boldsymbol{\delta}\boldsymbol{\alpha} + \boldsymbol{\delta}\boldsymbol{\omega} \tag{11}$$

where $\boldsymbol{\delta}\boldsymbol{\omega} \equiv \boldsymbol{\omega} - \hat{\boldsymbol{\omega}}$. From Eq. (7) we have

$$\begin{aligned} \boldsymbol{\omega} &= (I_{3\times3}-S)\tilde{\boldsymbol{\omega}} - (I_{3\times3}-S)\mathbf{b} - (I_{3\times3}-S)\boldsymbol{\eta}_v \\ \hat{\boldsymbol{\omega}} &= (I_{3\times3}-\hat{S})\tilde{\boldsymbol{\omega}} - (I_{3\times3}-\hat{S})\hat{\mathbf{b}} \end{aligned} \tag{12}$$

Then $\boldsymbol{\delta}\boldsymbol{\omega}$ is given by

$$\begin{aligned} \boldsymbol{\delta}\boldsymbol{\omega} = &-\Delta S\,\tilde{\boldsymbol{\omega}} - \Delta\mathbf{b} + (\Delta S + \hat{S})(\Delta\mathbf{b} + \hat{\mathbf{b}}) - \hat{S}\,\hat{\mathbf{b}} \\ &-(I_{3\times3} - \hat{S} - \Delta S)\boldsymbol{\eta}_v \end{aligned} \tag{13}$$

where $\Delta S \equiv S - \hat{S}$ and $\Delta\mathbf{b} \equiv \mathbf{b} - \hat{\mathbf{b}}$. Ignoring second-order terms leads to

$$
\begin{aligned}
\boldsymbol{\delta\omega} &= \left(I_{3\times3} - \hat{S}\right)\Delta\mathbf{b} - \mathrm{diag}\left(\tilde{\boldsymbol{\omega}} - \hat{\mathbf{b}}\right)\Delta\mathbf{s} \\
&\quad -\hat{U}\,\Delta\mathbf{k}_U - \hat{L}\,\Delta\mathbf{k}_L - \left(I_{3\times3} - \hat{S}\right)\boldsymbol{\eta}_v \\
\hat{U} &= \begin{bmatrix} \tilde{\omega}_2 - \hat{b}_2 & \tilde{\omega}_3 - \hat{b}_3 & 0 \\ 0 & 0 & \tilde{\omega}_3 - \hat{b}_3 \\ 0 & 0 & 0 \end{bmatrix} \\
\hat{L} &= \begin{bmatrix} 0 & 0 & 0 \\ \tilde{\omega}_1 - \hat{b}_1 & 0 & 0 \\ 0 & \tilde{\omega}_1 - \hat{b}_1 & \tilde{\omega}_2 - \hat{b}_2 \end{bmatrix}
\end{aligned}
\tag{14}
$$

where diag denotes a diagonal matrix, $\Delta\mathbf{s}$ is a vector of the diagonal elements of ΔS, and $\Delta\mathbf{k}_U$ and $\Delta\mathbf{k}_L$ correspond to the upper and lower off-diagonal elements of ΔS. Hence, the matrices $F(t)$, $G(t)$ and $Q(t)$ are given by

$$
\begin{aligned}
F &= \begin{bmatrix} -\left[\hat{\boldsymbol{\omega}}\times\right] & -\left(I_{3\times3} - \hat{S}\right) & \mathrm{diag}\left(\tilde{\boldsymbol{\omega}} - \hat{\mathbf{b}}\right) & \hat{U} & \hat{L} \\ 0_{3\times3} & 0_{3\times3} & 0_{3\times3} & 0_{3\times3} & 0_{3\times3} \\ 0_{3\times3} & 0_{3\times3} & 0_{3\times3} & 0_{3\times3} & 0_{3\times3} \\ 0_{3\times3} & 0_{3\times3} & 0_{3\times3} & 0_{3\times3} & 0_{3\times3} \\ 0_{3\times3} & 0_{3\times3} & 0_{3\times3} & 0_{3\times3} & 0_{3\times3} \end{bmatrix} \\
G &= \begin{bmatrix} -\left(I_{3\times3} - \hat{S}\right) & 0_{3\times3} & 0_{3\times3} & 0_{3\times3} & 0_{3\times3} \\ 0_{3\times3} & I_{3\times3} & 0_{3\times3} & 0_{3\times3} & 0_{3\times3} \\ 0_{3\times3} & 0_{3\times3} & I_{3\times3} & 0_{3\times3} & 0_{3\times3} \\ 0_{3\times3} & 0_{3\times3} & 0_{3\times3} & I_{3\times3} & 0_{3\times3} \\ 0_{3\times3} & 0_{3\times3} & 0_{3\times3} & 0_{3\times3} & I_{3\times3} \end{bmatrix} \\
Q &= \begin{bmatrix} \sigma_v^2 I_{3\times3} & 0_{3\times3} & 0_{3\times3} & 0_{3\times3} & 0_{3\times3} \\ 0_{3\times3} & \sigma_u^2 I_{3\times3} & 0_{3\times3} & 0_{3\times3} & 0_{3\times3} \\ 0_{3\times3} & 0_{3\times3} & \sigma_s^2 I_{3\times3} & 0_{3\times3} & 0_{3\times3} \\ 0_{3\times3} & 0_{3\times3} & 0_{3\times3} & \sigma_U^2 I_{3\times3} & 0_{3\times3} \\ 0_{3\times3} & 0_{3\times3} & 0_{3\times3} & 0_{3\times3} & \sigma_L^2 I_{3\times3} \end{bmatrix}
\end{aligned}
\tag{15}
$$

Table 1. EKF For Attitude Estimation

Initialize	$\hat{\mathbf{q}}(t_0)=\hat{\mathbf{q}}_0,\quad \hat{\mathbf{b}}(t_0)=\hat{\mathbf{b}}_0,\quad \hat{\mathbf{s}}(t_0)=\hat{\mathbf{s}}_0$ $\hat{\mathbf{k}}_U(t_0)=\hat{\mathbf{k}}_{U0},\quad \hat{\mathbf{k}}_L(t_0)=\hat{\mathbf{k}}_{L0}$ $P(t_0)=P_0$
Compute Gain	$K_k=P_k^- H^T\left(H\,P_k^- H^T+R_k\right)^{-1}$ $H=\begin{bmatrix} I_{3\times3} & 0_{3\times3} & 0_{3\times3} & 0_{3\times3} & 0_{3\times3}\end{bmatrix}$
Update	$P_k^+=\left(I_{15\times15}-K_kH\right)P_k^-$ $\Delta\hat{\mathbf{x}}_k^+=2K_k\,\Xi^T\left(\hat{\mathbf{q}}_k^-\right)\tilde{\mathbf{q}}_k$ $\Delta\hat{\mathbf{x}}_k^+\equiv\begin{bmatrix}\boldsymbol{\delta\hat{\alpha}}_k^{+T} & \Delta\hat{\mathbf{b}}_k^{+T} & \Delta\hat{\mathbf{s}}_k^{+T} & \Delta\hat{\mathbf{k}}_{Uk}^{+T} & \Delta\hat{\mathbf{k}}_{Lk}^{+T}\end{bmatrix}^{TT}$ $\hat{\mathbf{q}}_k^+=\hat{\mathbf{q}}_k^-+\frac{1}{2}\Xi\left(\hat{\mathbf{q}}_k^-\right)\boldsymbol{\delta\hat{\alpha}}_k^{+T}$, re-normalize $\hat{\mathbf{b}}_k^+=\hat{\mathbf{b}}_k^-+\Delta\hat{\mathbf{b}}_k^+$ $\hat{\mathbf{s}}_k^+=\hat{\mathbf{s}}_k^-+\Delta\hat{\mathbf{s}}_k^+$ $\hat{\mathbf{k}}_{Uk}^+=\hat{\mathbf{k}}_{Uk}^-+\Delta\hat{\mathbf{k}}_{Uk}^+$ $\hat{\mathbf{k}}_{Lk}^+=\hat{\mathbf{k}}_{Lk}^-+\Delta\hat{\mathbf{k}}_{Lk}^+$
Propagate	$\hat{\boldsymbol{\omega}}(t)=\left[I_{3\times3}-\hat{S}(t)\right]\left[\tilde{\boldsymbol{\omega}}(t)-\hat{\mathbf{b}}(t)\right]$ $\dot{\hat{\mathbf{q}}}=\frac{1}{2}\Xi\left[\hat{\mathbf{q}}(t)\right]\hat{\boldsymbol{\omega}}(t)$ $\dot{\hat{\mathbf{b}}}(t)=\mathbf{0}$ $\dot{\hat{\mathbf{s}}}(t)=\mathbf{0}$ $\dot{\hat{\mathbf{k}}}_U=\mathbf{0}$ $\dot{\hat{\mathbf{k}}}_L=\mathbf{0}$ $\dot{P}(t)=F(t)P(t)+P(t)F^T(t)+G(t)Q(t)G^T(t)$

A discrete-time propagation of the quaternion and error-covariance is possible (see [5] for details). The discrete-time covariance propagation is given by

$$P_k^-=\Phi_k P_k^+\Phi_k^T+Q_k \tag{16}$$

where Φ_k and Q_k are discrete-time state transition and process-noise covariance matrices, respectively. For small sampling intervals the discrete process noise matrix is well approximated by (also see [8])

$$\Phi_k \approx I_{15\times 15} + \Delta t\, F(t) + \frac{1}{2}\Delta t^2\, F^2(t)$$

$$Q_k \approx \begin{bmatrix} \left(\sigma_v^2 + \frac{1}{3}\sigma_u^2\Delta t^2\right)\Delta t\, I_{3\times 3} + \frac{1}{3}\sigma_s^2\Delta t^3\Omega^2\left(\hat{\boldsymbol{\omega}}_k\right) & -\frac{1}{2}\sigma_u^2\Delta t^2 I_{3\times 3} & -\frac{1}{2}\sigma_s^2\Delta t^2\Omega^2\left(\hat{\boldsymbol{\omega}}_k\right) & \frac{1}{2}\sigma_U^2\Delta t^2\hat{U} & \frac{1}{2}\sigma_L^2\Delta t^2\hat{L} \\ -\frac{1}{2}\sigma_u^2\Delta t^2 I_{3\times 3} & \sigma_u^2\Delta t^2 I_{3\times 3} & 0_{3\times 3} & 0_{3\times 3} & 0_{3\times 3} \\ -\frac{1}{2}\sigma_s^2\Delta t^2\Omega^2\left(\hat{\boldsymbol{\omega}}_k\right) & 0_{3\times 3} & \sigma_v^2\Delta t^2 I_{3\times 3} & 0_{3\times 3} & 0_{3\times 3} \\ \frac{1}{2}\sigma_U^2\Delta t^2\hat{U}^T & 0_{3\times 3} & 0_{3\times 3} & \sigma_U^2\Delta t^2 I_{3\times 3} & 0_{3\times 3} \\ \frac{1}{2}\sigma_L^2\Delta t^2\hat{L}^T & 0_{3\times 3} & 0_{3\times 3} & 0_{3\times 3} & \sigma_L^2\Delta t^2 I_{3\times 3} \end{bmatrix} \tag{17}$$

where Δt is the sampling interval and $\Omega\left(\hat{\boldsymbol{\omega}}_k\right)$ is a diagonal matrix made up of the elements of the estimate rate.

3.0 Multiple-Model Adaptive Estimation

3.1 MMAE Formulation

Multiple-model adaptive estimation described in [2] is a recursive estimator that uses a bank of filters that depend on some unknown parameters. In our case these parameters are the process noise covariance, denoted by the vector $\mathbf{p}$, which is assumed to be constant (at least throughout the interval of adaptation). Note that we do not necessarily need to make the stationary assumption for the state and/or output processes though, i.e. time varying state and output matrices can be used. A set of distributed elements is generated from some known probability density function (pdf) of $\mathbf{p}$, denoted by $p(\mathbf{p})$, to give $\left\{\mathbf{p}^{(\ell)}; \ell = 1,\ldots,M\right\}$. The goal of the estimation process is to determine the conditional pdf of the ℓ^{th} element of $\mathbf{p}^{(\ell)}$ given the current-time measurement $\tilde{\mathbf{y}}_k$. Application of Bayes rule yields

$$p\left(\mathbf{p}^{(\ell)} \mid \tilde{\mathbf{Y}}_k\right) = \frac{p\left(\tilde{\mathbf{Y}}_k \mid \mathbf{p}^{(\ell)}\right) p\left(\mathbf{p}^{(\ell)}\right)}{\sum_{j=1}^{M} p\left(\tilde{\mathbf{Y}}_k \mid \mathbf{p}^{(j)}\right) p\left(\mathbf{p}^{(j)}\right)} \tag{18}$$

where $\tilde{\mathbf{Y}}_k$ denotes the sequence $\{\tilde{\mathbf{y}}_0, \tilde{\mathbf{y}}_1, \ldots, \tilde{\mathbf{y}}_k\}$. The *a posteriori* probabilities can be computed through

$$p\left(\mathbf{p}^{(\ell)} \mid \tilde{\mathbf{Y}}_k\right) = \frac{p\left(\tilde{\mathbf{y}}_k, \mathbf{p}^{(\ell)} \mid \tilde{\mathbf{Y}}_{k-1}\right)}{p\left(\tilde{\mathbf{y}}_k \mid \tilde{\mathbf{Y}}_{k-1}\right)} = \frac{p\left(\tilde{\mathbf{y}}_k \mid \hat{\mathbf{x}}_k^{-(\ell)}\right) p\left(\mathbf{p}^{(\ell)} \mid \tilde{\mathbf{Y}}_{k-1}\right)}{\sum_{j=1}^{M} p\left(\tilde{\mathbf{y}}_k \mid \hat{\mathbf{x}}_k^{-(j)}\right) p\left(\mathbf{p}^{(j)} \mid \tilde{\mathbf{Y}}_{k-1}\right)} \tag{19}$$

where $\hat{\mathbf{x}}_k^{-(\ell)}$ denotes the propagated state estimate of the ℓ^{th} Kalman filter. Note that the denominator of Eq. (19) is just a normalizing factor to ensure that $p\left(\mathbf{p}^{(\ell)} \mid \tilde{\mathbf{Y}}_k\right)$ is a pdf. The recursion formula can now be cast into a set of defined weights $\varpi_k^{(\ell)}$

$$\begin{aligned} \varpi_k^{(\ell)} &= \varpi_{k-1}^{(\ell)} \, p\left(\tilde{\mathbf{y}}_k \mid \hat{\mathbf{x}}_k^{-(\ell)}\right) \\ \varpi_k^{(\ell)} &\leftarrow \frac{\varpi_k^{(\ell)}}{\sum_{j=1}^{M} \varpi_k^{(\ell)}} \end{aligned} \tag{20}$$

where $\varpi_k^{(\ell)} \equiv p\left(\mathbf{p}^{(\ell)} \mid \tilde{\mathbf{Y}}_{k-1}\right)$. The weights are initialized to $\varpi_0^{(\ell)} = 1/M$ for $\ell = 1, 2, \ldots, M$. Note that $p\left(\tilde{\mathbf{y}}_k \mid \hat{\mathbf{x}}_k^{-(\ell)}\right)$ denotes the likelihood function.

The conditional mean estimate is the weighted sum of the parallel filter estimates

$$\hat{\mathbf{x}}_k^{-} = \sum_{j=1}^{M} \varpi_k^{(j)} \hat{\mathbf{x}}_k^{-(j)} \tag{21}$$

Also, the error covariance of the state estimate can be computed using

$$P_k^- = \sum_{j=1}^{M} \varpi_k^{(j)} \left(\hat{\mathbf{x}}_k^{-(j)} - \hat{\mathbf{x}}_k^- \right) \left(\hat{\mathbf{x}}_k^{-(j)} - \hat{\mathbf{x}}_k^- \right)^T \tag{22}$$

The specific estimate for $\mathbf{p}$ at time t_k, denoted by $\hat{\mathbf{p}}_k$, and error covariance, denoted by Z_k, are given by

$$\hat{\mathbf{p}}_k = \sum_{j=1}^{M} \varpi_k^{(j)} \mathbf{p}^{(j)} \tag{23a}$$

$$Z_k = \sum_{j=1}^{M} \varpi_k^{(j)} \left(\mathbf{p}^{(j)} - \hat{\mathbf{p}}_k \right) \left(\mathbf{p}^{(j)} - \hat{\mathbf{p}}_k \right)^T \tag{23b}$$

Equation (23b) can be used to define 3σ bounds on the estimate $\hat{\mathbf{p}}_k$.

3.2 Attitude Likelihood Function

This section derives the likelihood function for the MMAE algorithm using quaternion measurements. From Table 1, the measurement residual is defined to be (ignoring the propagated notation for $\hat{\mathbf{q}}$)

$$\mathbf{e} \equiv 2\Xi^T \left(\hat{\mathbf{q}} \right) \tilde{\mathbf{q}} \tag{24}$$

which is derived from the vector part of $\tilde{\mathbf{q}} \otimes \hat{\mathbf{q}}^{-1}$ (the factor of 2 is used so that $\mathbf{e}$ represents half-angle residuals). Using Eq. (9) and $\hat{\mathbf{q}} = \mathbf{q} + \frac{1}{2}\Xi^T \left(\mathbf{q} \right) \boldsymbol{\delta\alpha}$ in Eq. (24) gives

$$\mathbf{e} = 2\left[\Xi^T \left(\mathbf{q} \right) + \frac{1}{2}\Xi^T \left(\Xi(\mathbf{q}) \boldsymbol{\delta\alpha} \right) \right] \left[\mathbf{q} + \frac{1}{2}\Xi^T \left(\mathbf{q} \right) \mathbf{v} \right] \tag{25}$$

Using the identity $\Xi^T(\mathbf{q})\Xi(\mathbf{q})\boldsymbol{\delta\alpha}\big) = -[\boldsymbol{\delta\alpha}\times]\Xi^T(\mathbf{q}) - \boldsymbol{\delta\alpha}\,\mathbf{q}^T$ in Eq. (25) leads to

$$\mathbf{e} = \mathbf{v} - \frac{1}{2}[\boldsymbol{\delta\alpha}\times]\mathbf{v} - \boldsymbol{\delta\alpha} \tag{26}$$

where $\Xi^T(\mathbf{q})\Xi(\mathbf{q}) = I_{3\times 3}$, $\Xi^T(\mathbf{q})\mathbf{q} = \mathbf{0}$ and $\mathbf{q}^T\mathbf{q} = 1$ have been used. Therefore, since $\boldsymbol{\delta\alpha}$ and $\mathbf{v}$ are uncorrelated, the covariance of the residual at time t_k, using the propagated values, is given by

$$E\left\{\mathbf{e}_k^-\mathbf{e}_k^{-T}\right\} = H\,P_k^-H^T + R_k \tag{27}$$

where H is defined in Table 1. Therefore the likelihood function is given by

$$\Lambda_\ell \equiv p\left(\tilde{\mathbf{y}}_k \mid \hat{\mathbf{x}}_k^{-(\ell)}\right) = \frac{1}{\left\{\det\left[2\pi\left(H\,P_k^{-(\ell)}H^T + R_k\right)\right]\right\}^{1/2}}\exp\left[-\frac{1}{2}\mathbf{e}_k^{-(\ell)}\left(H\,P_k^{-(\ell)}H^T + R_k\right)^{-1}\mathbf{e}_k^{-(\ell)}\right] \tag{28}$$

which is used to update the weights in the MMAE algorithm.

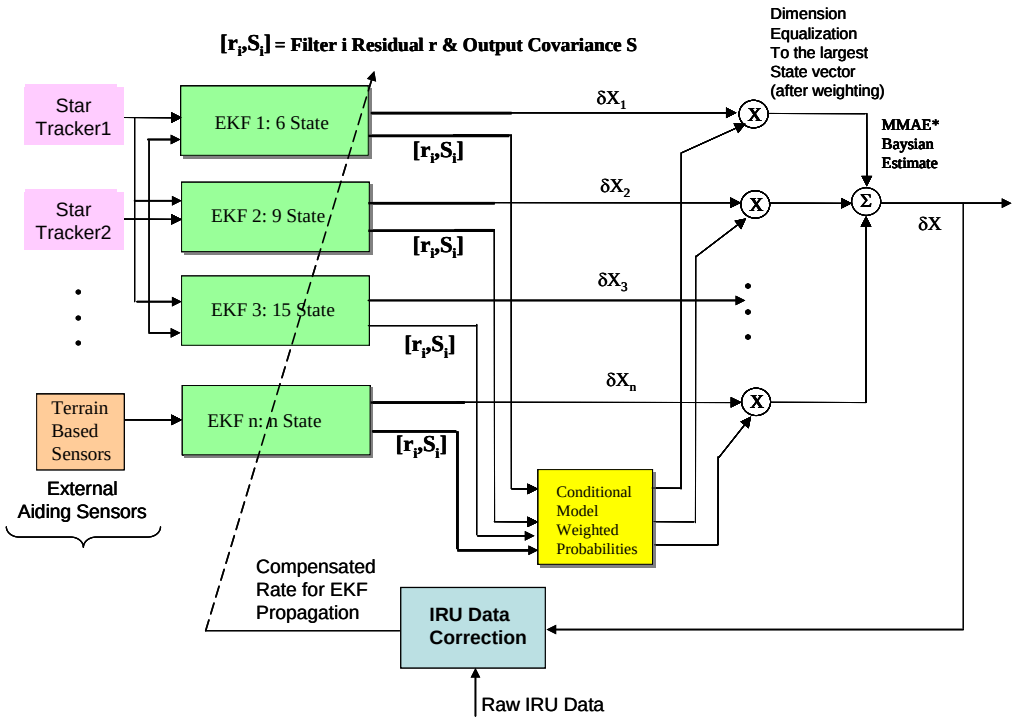

Figure 5: MMAE Architecture Suitable for Multiple External Aiding Sensors

4.0 Performance Evaluation

4.1 15 State Single EKF Performance Using CMOS Star Tracker & QRS MEMS Gyros

The CMOS star tracker attitude accuracy is at 70 arcsecs while the QRS gyros ARW is at 0.035 deg/hr^0.5. The mixing of gyros and CMOS star tracker will provide continuous high rate attitude and rate information with better quality information thanks to the EKF calibration filter to remove the gyros' error sources and the CMOS star tracker's high noise (75 arcseconds).

The attitude estimation accuracy of a single 15 state EKF is presented in Figure 6. The single EKF calibration filter has reduced the CMOS star tracker attitude from 75 arcseconds down to **[28.5052 24.6240 29.0859] arcsecs, 1 sigma.**

Figures 7, 8, 9, and 10 present the EKF performance of MEMS gyros' error sources (bias errors, scale factor errors, and mis-alignment errors)

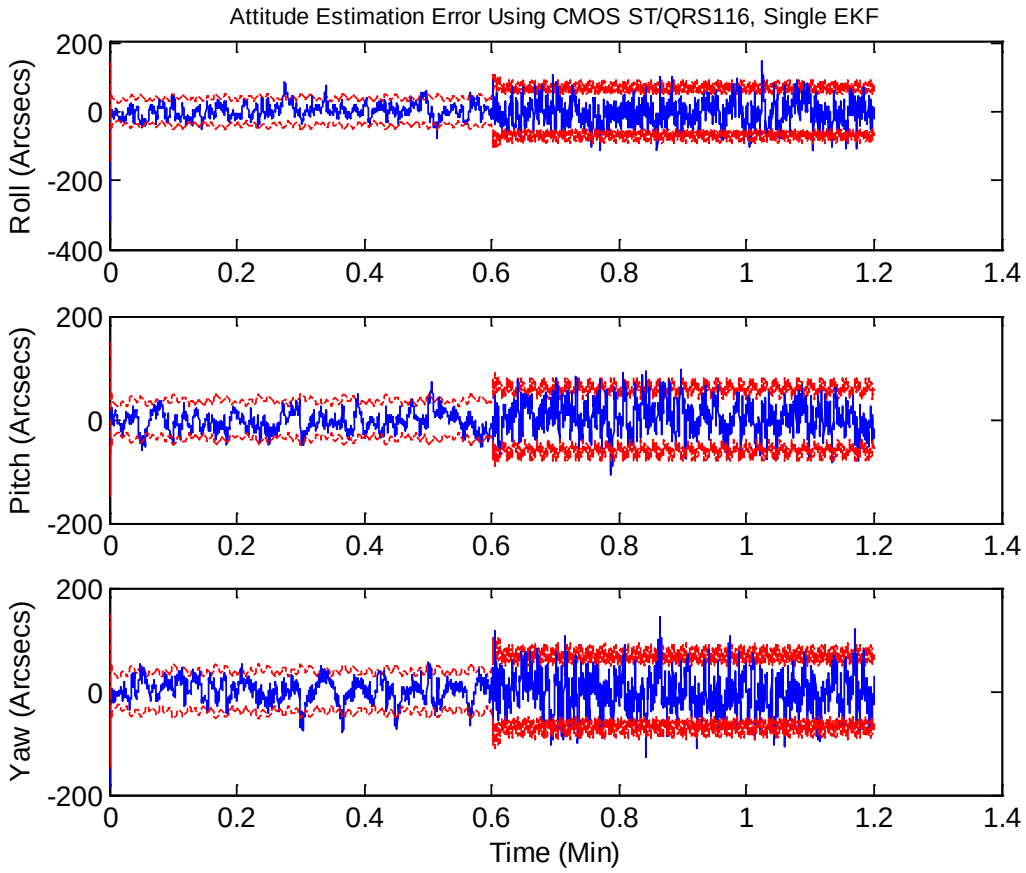

Figure 6: Single EKF Performance, 1sigma=[28.5052 24.6240 29.0859] arcsecs

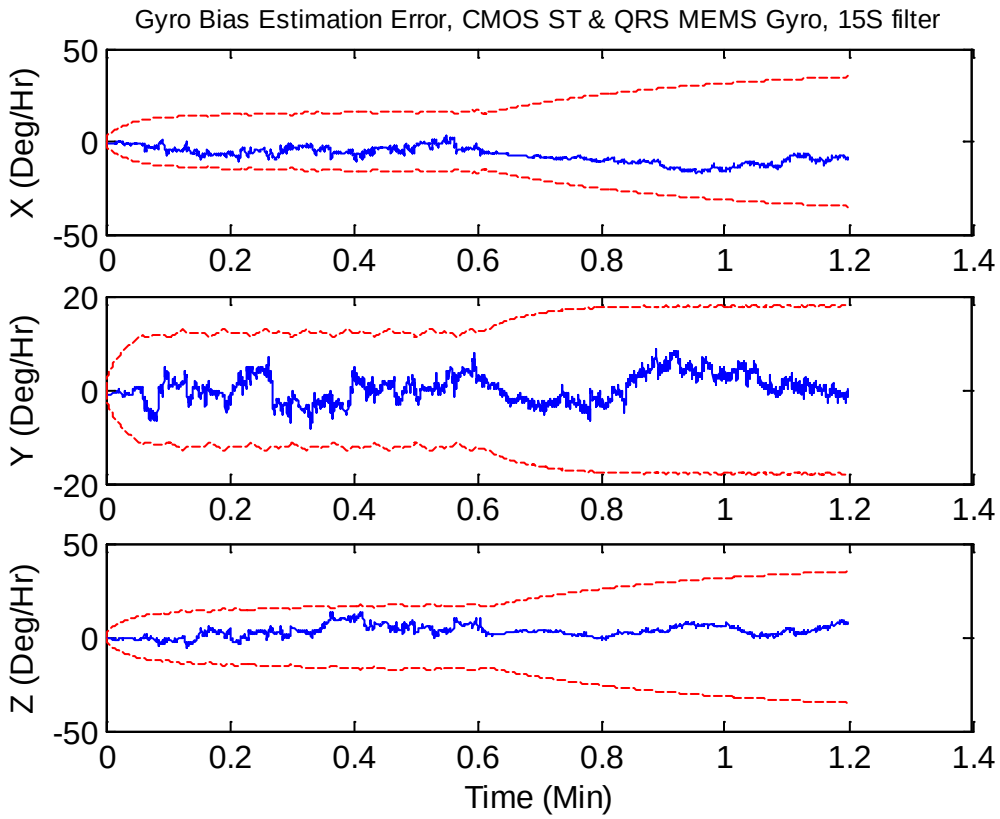

Figure 7: Gyros Bias Errors Estimation Performance Via 15 State EKF

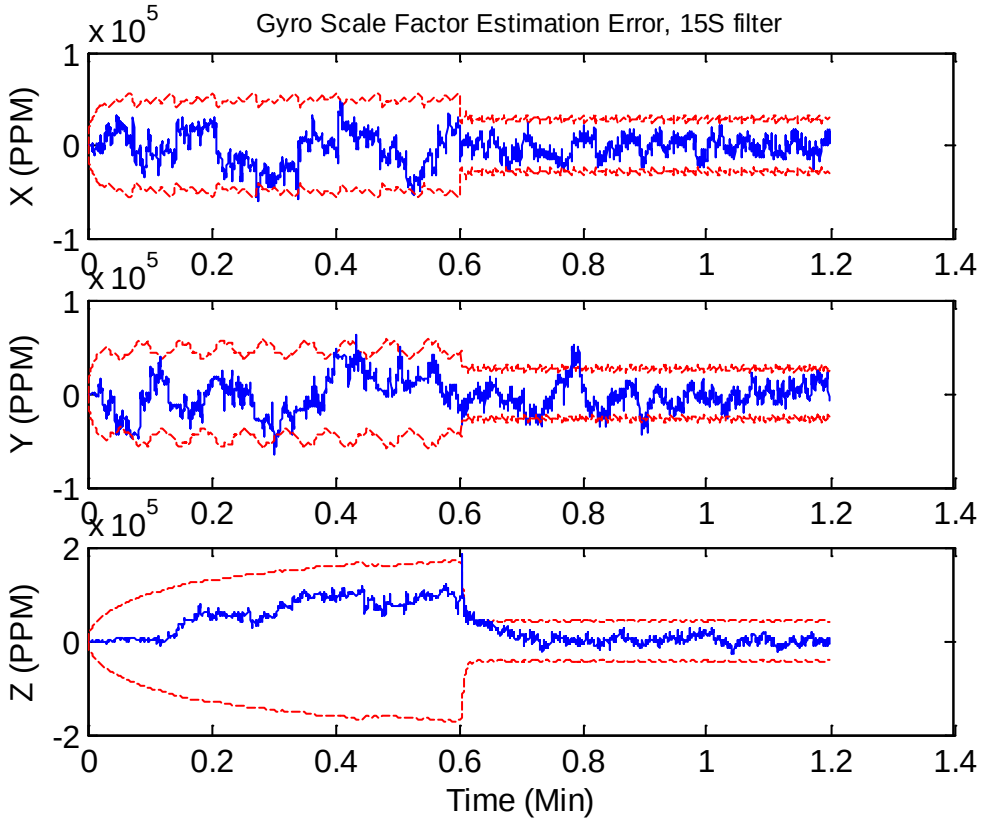

Figure 8: Gyros Scale Factor Errors Estimation Performance Via 15 State EKF

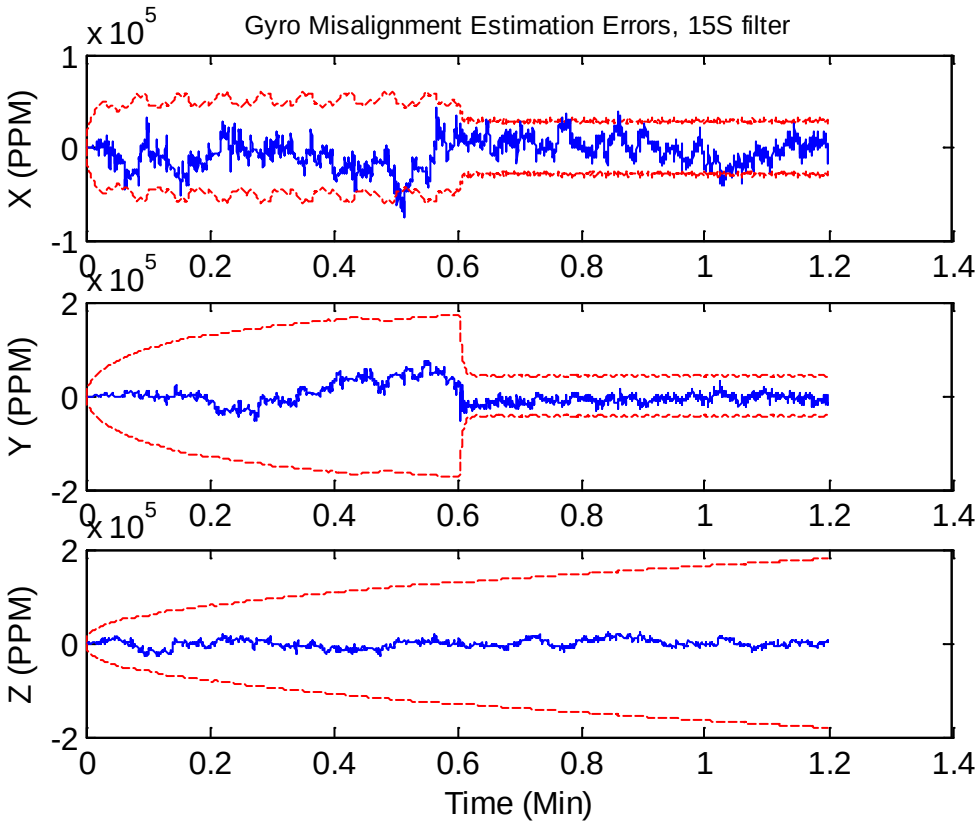

Figure 9: Gyros Upper Mis-Alignment Errors Estimation Performance Via 15 State EKF

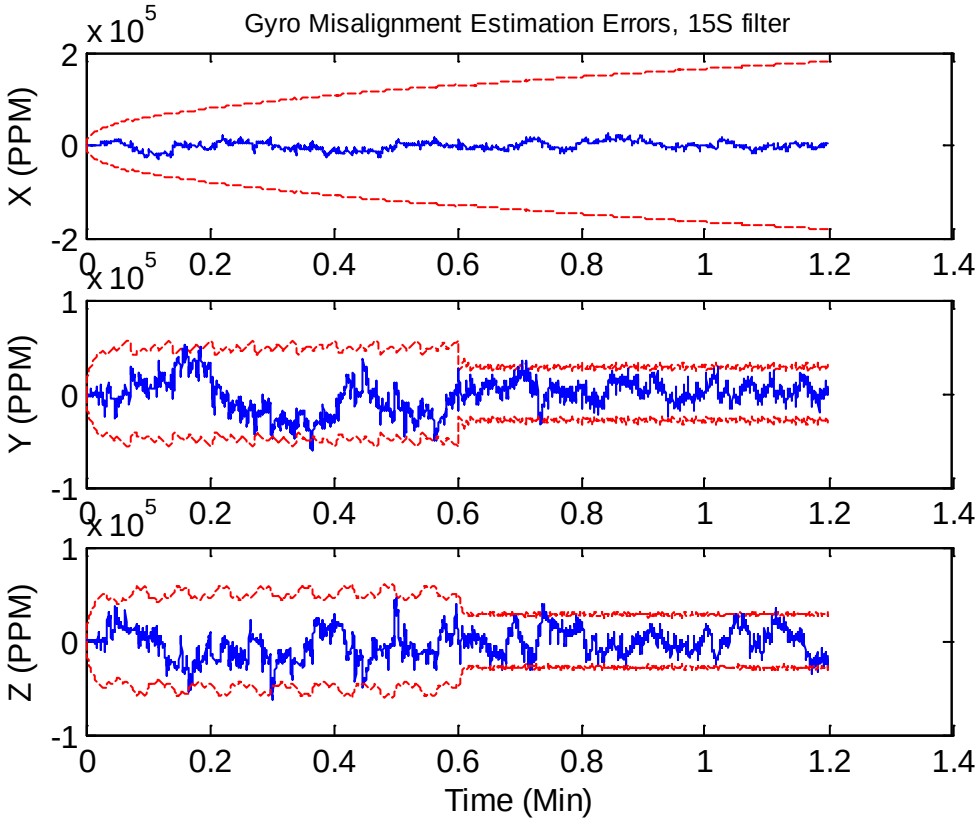

Figure 10: Gyros Lower Mis-Alignment Errors Estimation Performance Via 15 State EKF

4.2 MMAE Performance Using CMOS Star Tracker & QRS MEMS Gyros

The MMAE as expected has outperformed the single 15 state EKF. The mixing of three EKFs, 6 state, 9 state, and 15 state has produced better attitude estimation as shown in Figure 11. The accuracy improvement is almost five times better. (i.e., 1 sigma=[5.6423 5.0104 5.3456] arcsecs).

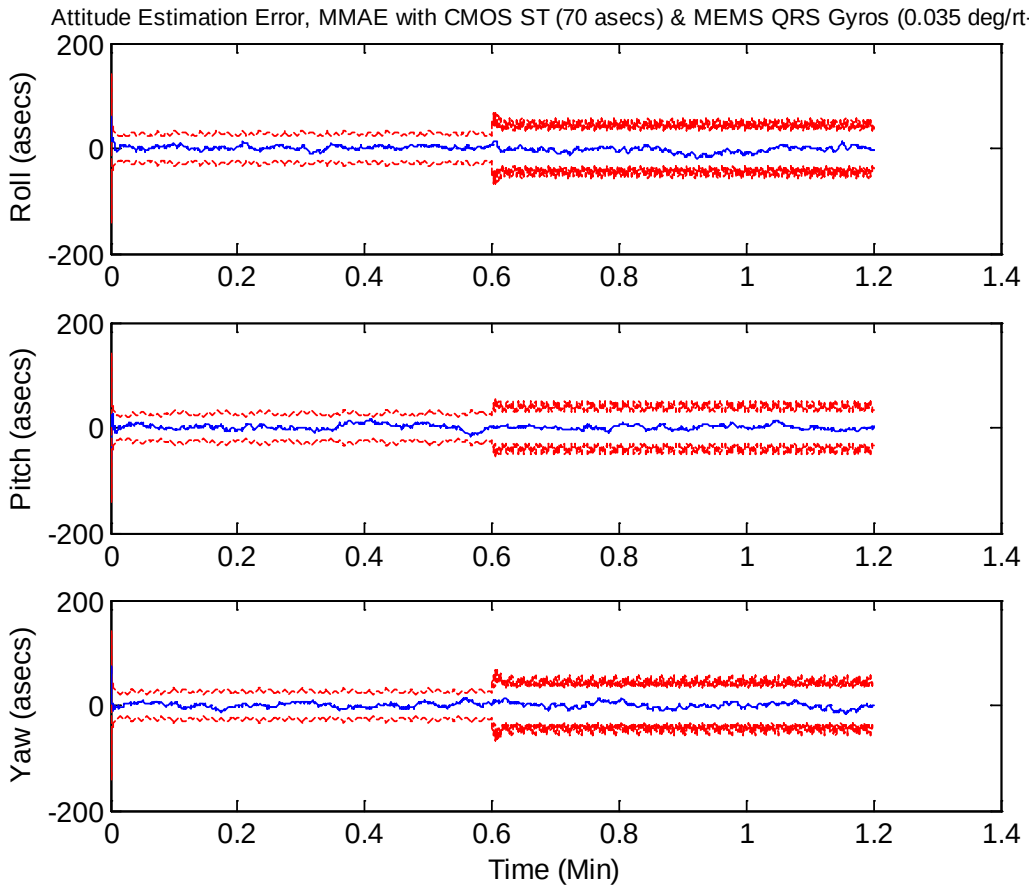

Figure 11: Attitude Estimation Performance Using the MMAE. 1 sigma=[5.6423 5.0104 5.3456] arcsecs

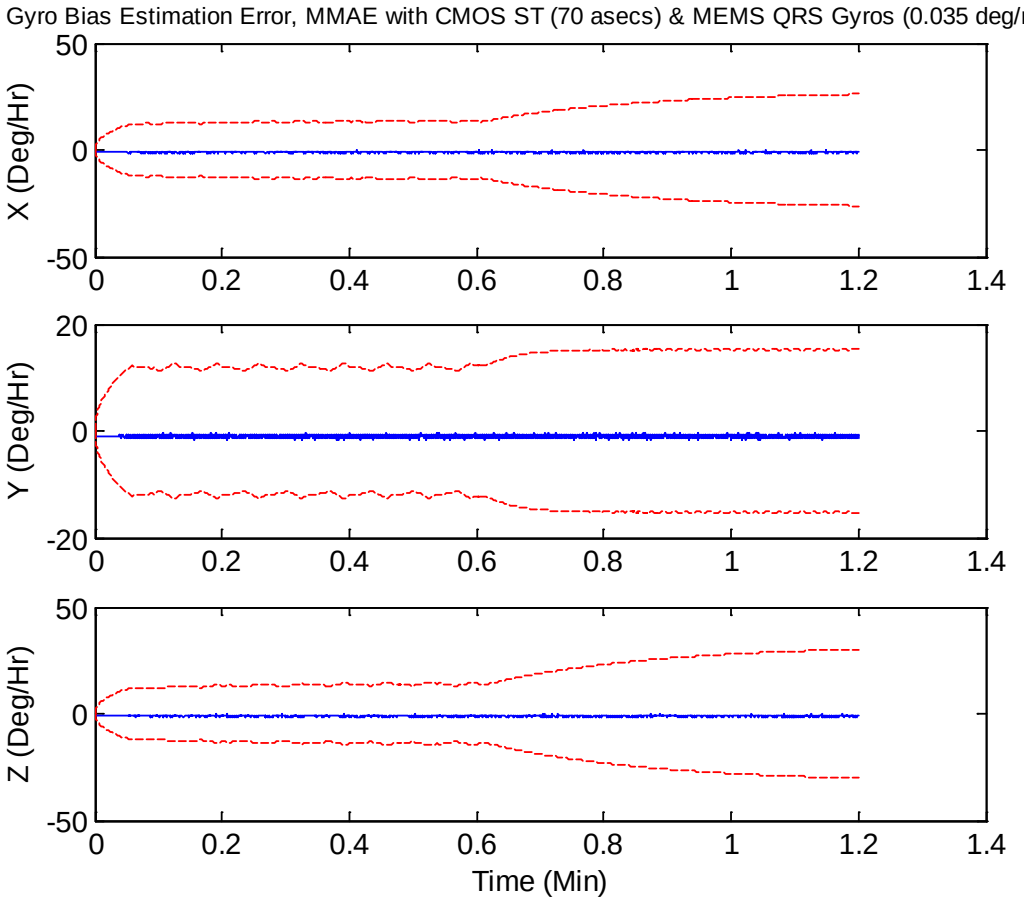

Figure 12: Gyros Bias Errors Estimation Performance Via MMAE

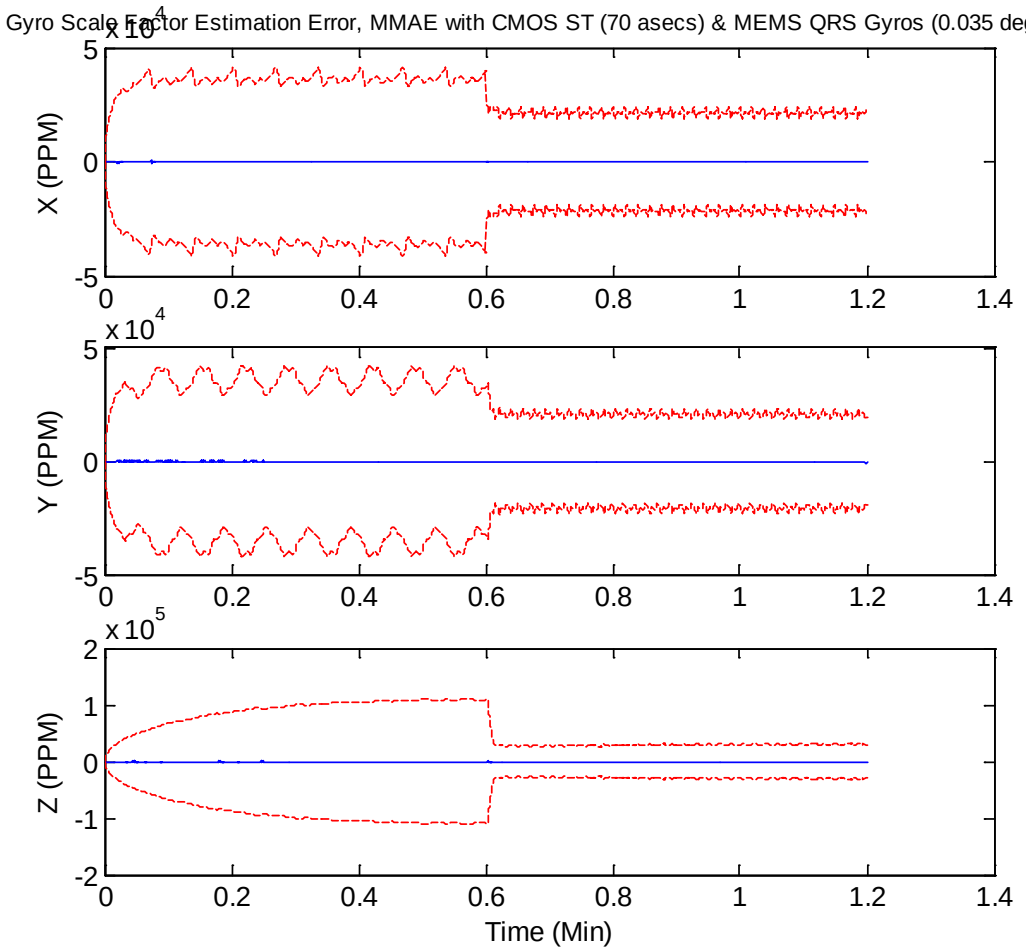

Figure 13: Gyros Scale Factor Errors Estimation Performance Via MMAE

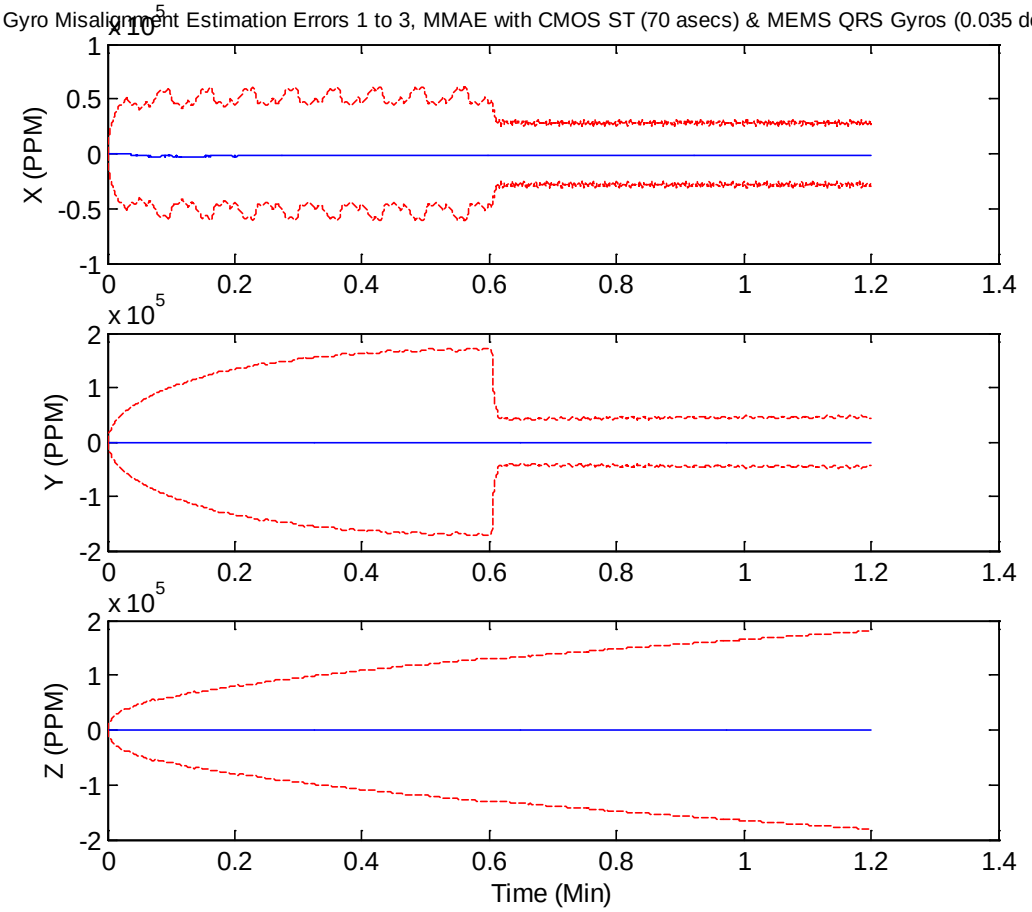

Figure 14: Gyros Upper Mis-Alignment Errors Estimation Performance Via MMAE

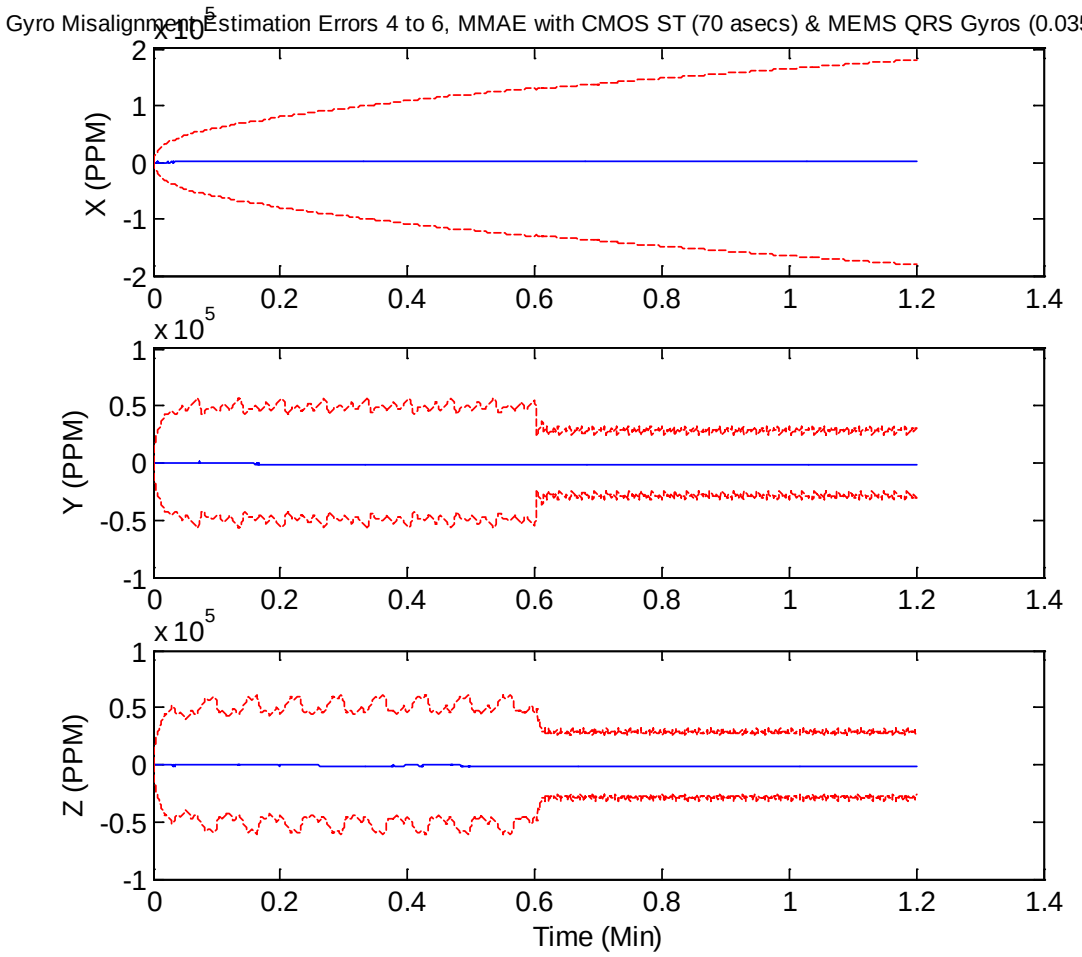

Figure 15: Gyros Lower Mis-Alignment Errors Estimation Performance Via MMAE

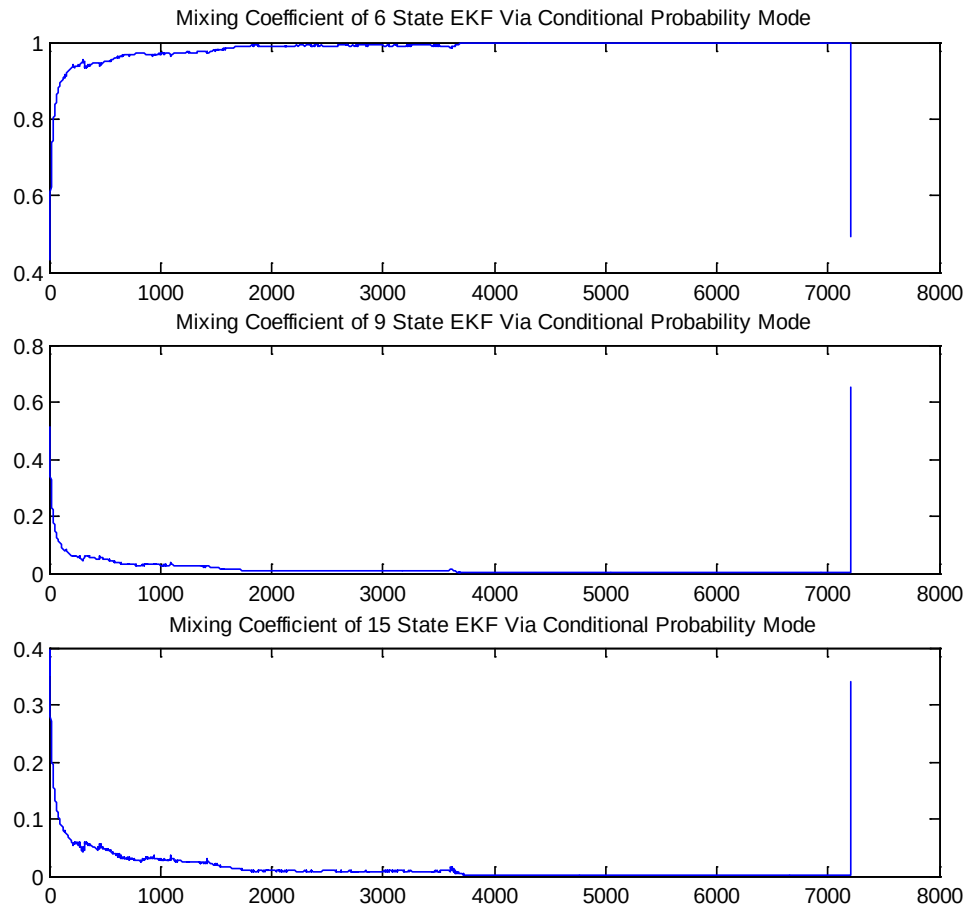

Figure 16: MMAE Mixing Coefficients

4.3 Gyros Noise Estimation for Update and Cancellation

Figure 16 presents the excellent gyro noise identification using the MMAE scheme implemented as a separate subsystem to estimate the IRU noise. Only rate random walk (RRW) and angular random walk (ARW) are estimated in this study. The one sigma values of RRW and ARW noises estimated online, will feed the adaptive process noise block to compute the right signature for the MMAE/IMM filter to effectively maintain the accuracy of the navigation solution in the presence of IRU performance degradation (due to aging or in-orbit drift variation)

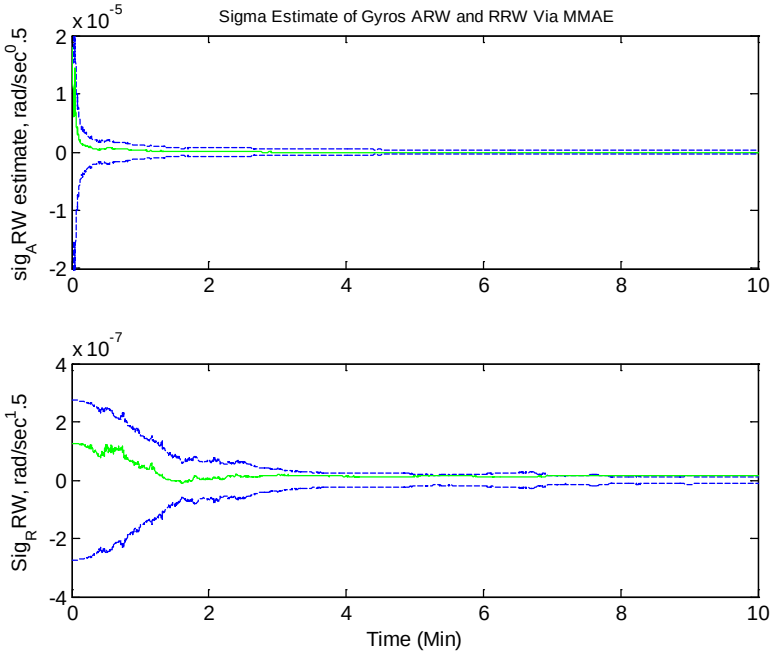

Figure 17. RRW and ARW Noise Estimation

5.0 Conclusion

An adaptive filtering architecture via MMAE scheme has been developed and experimented for the possibility of using low cost low grade MEMS gyros and CMOS star tracker (lower grade than a traditional expensive high performance CCD star tracker) to produce precision attitude determination system. The proposed MMAE coupled with gyros noise estimation for update and cancellation is capable of ameliorating the effect of MEMS gyros bias, SF and MA errors while a traditional single EKF scheme suffers for a same operating condition. The MMAE scheme is exploited to offer two primary design features: (1) multiple EKF models mixing to provide the right fusion combination between various filter models' state vectors for a consistent navigation solution update at various rate magnitudes and (2) the ability to mix multiple external sensor data update in a simultaneous fashion via MMAE framework regardless their disparate update rate. In other words, external data available out of each sensor provided at different output rate can be systematically combined via the MMAE/IMM mixing scheme. Simulation performance results indicate that the MMAE/IMM provides better estimates compared to using each filter alone. Also, the MMAE approach is an effective scheme to estimate MEMS gyros noise parameters while not requiring an expensive CCD star tracker.

References:

1. Lefferts, E. J., Markley, F. L., and Shuster, M. D., "Kalman Filtering for Spacecraft Attitude Estimation," *Journal of Guidance, Control, and Dynamics*, Vol. 5, No. 5, 1982, pp. 417–429.

2. Lam, Q. M. and Crassidis, J. L., "Precision Attitude Determination Using A Multiple Model Adaptive Estimation Scheme," *Proceedings of the IEEE Aerospace Conference*, Big Sky, Montana, March 2007.

3. Markley, F.L., Cheng, Y., Crassidis, J.L., and Oshman, Y., "Averaging Quaternions," *Journal of Guidance, Control, and Dynamics*, Vol. 30, No. 4, 2007, pp. 1193-1197.

4. Bar-Shalom, Y. and Li, R., *Estimation and Tracking: Principles, Techniques, and Softwares*, Artech House, 1993.

5. Lam, Q. M., Li, X. R., and Fujikawa, S.J., "Future Trends to Enhance the Robustness of a Target Tracker," *Proceedings of the AIAA GN&C Conference*, San Diego, CA July 1996.

6. Shuster, M. D., "A Survey of Attitude Representations," *Journal of the Astronautical Sciences*, Vol. 41, No. 4, 1993, pp. 439-517.

7. Lam., Q. M. and Crassidis, J. L., "Evaluation of a Multiple Model Adaptive Estimation Scheme for Space Vehicle's Enhanced Navigation Solution," AIAA GN&C Conference 2007